

1 **Duplication events downstream of *IRXI* cause North Carolina macular dystrophy at**  
2 **the MCDR3 locus**

3

4 Valentina Cipriani,<sup>1,2,3,§,\*</sup> Raquel S Silva,<sup>1,2,§</sup> Gavin Arno,<sup>1,2</sup> Nikolas Pontikos,<sup>1,3</sup> Ambreen  
5 Kalhor,<sup>1,2</sup> Sandra Valeina,<sup>4</sup> Inna Inashkina,<sup>5</sup> Mareta Audere,<sup>5,6</sup> Katrina Rutka,<sup>5,6</sup> Bernard  
6 Puech,<sup>7</sup> Michel Michaelides,<sup>1,2</sup> Veronica van Heyningen,<sup>1</sup> Baiba Lace,<sup>5,8</sup> Andrew R  
7 Webster,<sup>1,2,\*</sup> Anthony T Moore<sup>1,2,9,\*</sup>

8

9 <sup>1</sup>UCL Institute of Ophthalmology, London, UK, <sup>2</sup>Moorfields Eye Hospital, London, UK,  
10 <sup>3</sup>UCL Genetics Institute, London, UK, <sup>4</sup>Children's Clinical University Hospital, Riga,  
11 Latvia, <sup>5</sup>Latvian Biomedical Research and Study Centre, Riga, Latvia, <sup>6</sup>Riga Stradins  
12 University, Riga, Latvia <sup>7</sup>Exploration de la Vision et Neuro-Ophthalmologie, Centre  
13 Hospitalier Universitaire, Lille, France <sup>8</sup>Centre Hospitalier de l'Université Laval, Québec,  
14 Canada, <sup>9</sup>Ophthalmology Department, UCSF School of Medicine, San Francisco, CA,  
15 USA

16

17 <sup>§</sup>These authors contributed equally to this work

18 <sup>\*</sup>To whom correspondence should be addressed.

19

20 **Corresponding authors:** Valentina Cipriani, PhD, UCL Institute of Ophthalmology, 11-  
21 43 Bath Street, London, EC1V 9EL, United Kingdom; email: [v.cipriani@ucl.ac.uk](mailto:v.cipriani@ucl.ac.uk);  
22 phone: +44 (0)207 608 4042; fax: +44 (0)207 608 6830; Andrew R. Webster, MD (Res),  
23 FRCOphth, UCL Institute of Ophthalmology, 11-43 Bath Street, London, EC1V 9EL,

24 United Kingdom; email: [andrew.webster@ucl.ac.uk](mailto:andrew.webster@ucl.ac.uk); Anthony T. Moore, MA,  
25 FRCOphth, UCSF School of Medicine, Koret Vision Center, 10 Koret Way, San  
26 Francisco, California (USA); email: [tony.moore@ucsf.edu](mailto:tony.moore@ucsf.edu)

27 **Abstract**

28 Word count: 192/200

29 Autosomal dominant North Carolina macular dystrophy (NCMD) is believed to represent  
30 a failure of macular development. The disorder has been assigned by linkage to two loci,  
31 MCDR1 on chromosome 6q16 and MCDR3 on chromosome 5p15-p13. Recently, non-  
32 coding variants upstream of *PRDM13* and a large duplication including *IRX1* have been  
33 identified. However, the underlying disease-causing mechanism remains uncertain.  
34 Through a combination of sequencing studies, we report two novel overlapping  
35 duplications at the MCDR3 locus, in a gene desert downstream of *IRX1* and upstream of  
36 *ADAMTS16*. One duplication of 43 kb was identified in nine NCMD families (with  
37 evidence for a shared ancestral haplotype), and another one of 45 kb was found in a  
38 single family. The MCDR3 locus is thus refined to a shared region of 39 kb that contains  
39 DNase hypersensitive sites active at a restricted time window during retinal  
40 development. Publicly available data confirmed expression of *IRX1* and *ADAMTS16* in  
41 human fetal retina, with *IRX1* preferentially expressed in fetal macula. These findings  
42 represent a major advance in our understanding of the molecular genetics of NCMD at  
43 the MCDR3 locus and provide insights into the genetic pathways involved in human  
44 macular development.

45

46 **Abbreviations list**

47 aCGH – array comparative genomic hybridization

48 CNV – Copy number variant

49 IBD – Identical-by-descent

- 50 iPSC – Induced pluripotent stem cell
- 51 DHS – DNase hypersensitive site
- 52 HH – Homozygosity Haplotype
- 53 MCDR – Macular dystrophy region
- 54 NCMD – North Carolina macular dystrophy
- 55 PCR – Polymerase chain reaction
- 56 RCHH – Region with a Conserved Homozygosity Haplotype
- 57 SNP – Single-nucleotide polymorphism
- 58 SNV – Single nucleotide variant
- 59 SV – Structural variant
- 60 WGS – Whole-genome sequencing
- 61

## 62 **Introduction**

63

64 North Carolina macular dystrophy (NCMD) is a rare autosomal dominant disorder in  
65 which there is abnormal development of the macula, a crucial structure of the central  
66 retina responsible for central vision and colour perception<sup>1</sup>. Understanding the genetics of  
67 rare developmental macular conditions is key for unravelling the mechanism of  
68 development of this structure that is found only in higher primates within mammals<sup>1</sup>.  
69 NCMD shows fully penetrant inheritance and is considered a non-progressive disorder  
70 with a wide range of phenotypic manifestations, usually affecting both eyes  
71 symmetrically<sup>2,3</sup>. Phenotypic presentation varies from mild cases with drusen-like  
72 deposits covering the macular region but with little or no visual impairment, to severe  
73 cases with marked central chorioretinal atrophy and poor vision. Although generally non-  
74 progressive, complications associated with choroidal neovascularization can contribute to  
75 visual deterioration.

76 The molecular genetics of NCMD has been extensively investigated with the disorder  
77 being mapped to chromosome 6q16 (MCDR1, MIM:136550) in multiple families of  
78 different ethnic origins since the early 1990s<sup>4-10</sup>. A similar phenotype has been assigned  
79 to a second locus at 5p15-13 (MCDR3, MIM:608850)<sup>11,3</sup>. Interestingly, several studies  
80 reported evidence for ancestral haplotypes at the MCDR1 locus<sup>2,12,13</sup>. Early sequencing  
81 studies of the two disease intervals failed to identify exonic disease-causing variants<sup>2,14</sup>.  
82 More recently, three novel single nucleotide variants (SNVs) were identified in 11  
83 families at the MCDR1 locus, within a DNase1 hypersensitivity site (DHS), in the non-  
84 coding interval between *PRDM13* and the neighbouring overlapping genes

85 *CCNC/TSTD3*<sup>15</sup>. Two tandem duplications including the full coding region of *PRDM13*,  
86 with some additional upstream and downstream sequence included, were also  
87 identified<sup>15,16</sup>. One MCDR3-linked family of Danish origin<sup>3</sup> was found to carry a 900 kb  
88 tandem duplication<sup>15</sup> that includes the entire coding sequence of *IRX1*. However,  
89 duplications of *IRX1* have been observed in several normal individuals from the Database  
90 of Genome Variants<sup>15,17</sup> and the significance of this reported variant is uncertain. Thus,  
91 the causative mechanism at the 5p15-13 NCMD locus remains unclear.

92 In this report we present a combination of genomic investigations in a cohort of 18  
93 NCMD families. The aim of this study was to identify any causative molecular changes  
94 and mechanism of disease in these families.

95

## 96 **Results**

97

### 98 *Families and brief clinical phenotype description*

99 Eighteen families with phenotypes consistent with a diagnosis of NCMD were included  
100 in the study (Table 1 and Supplementary Fig. S1). Four families were previously  
101 reported: suggestive linkage at the MCDR3 locus has been recently described for family  
102 1<sup>14</sup>, family 2 was originally reported to be linked to the MCDR3 locus<sup>11</sup>, and families 12  
103 and 13 were linked to MCDR1<sup>7,9</sup>, with family 13 recently found to carry the SNV V2  
104 upstream of *PRDM13*<sup>15</sup>. All families (mostly of small size) showed autosomal dominant  
105 inheritance and had at least one individual with Grade 3 disease. DNA samples from a  
106 total of 56 affected and 33 unaffected family members were available for genetic  
107 analysis.

108 Figure 1 shows fundus autofluorescence and optical coherence tomography (OCT)  
109 images for selected individuals from families 2 and 3. Individual IV:5 from family 2  
110 presents with a well demarcated, relatively symmetrical, bilateral area of macular  
111 chorioretinal atrophy, while individual IV:3 from family 3 shows a mild form of disease  
112 with relatively symmetrical, bilateral hyperfluorescent drusen-like deposits concentrated  
113 in the macular region.

114

115 *Haplotype sharing analysis can exclude or suggest genetic mapping at known NCMD*  
116 *loci*

117 Haplotype sharing analysis was carried out using the Homozygosity Haplotype (HH)  
118 method<sup>18</sup> to search for shared identical-by-descent (IBD) chromosomal segments among  
119 affected individuals within each family. This analysis was performed in those families for  
120 which Illumina single-nucleotide polymorphism (SNP) array data were available for  
121 more than one affected family member (families 1-5 and 12-13). The 6q16 MCDR1 locus  
122 was excluded in four families, including the two previously MCDR3-linked families 1<sup>14</sup>  
123 and 2<sup>11</sup> and unreported families 3 and 4 (Supplementary Figs. S2-S5). Family 5 showed  
124 evidence for haplotype sharing at many regions across the genome, including both the  
125 6q16 and 5p15-p13 loci (Supplementary Fig. S6). The two previously reported MCDR1-  
126 linked families 12<sup>7</sup> and 13<sup>9</sup> were confirmed with evidence for a Region with a Conserved  
127 HH (RCHH) at the 6q16 locus, and not at the 5p15-p13 locus (Supplementary Figs. S7-  
128 S8).

129

130 *Two additional NCMD families shown to carry previously reported SNV upstream of*

131 ***PRDM13 at the MCDR1 locus***

132 All families, except families 1-4 for which linkage at the 6q16 locus had been excluded  
133 via haplotype sharing analysis, were tested with Sanger Sequencing for the three  
134 previously reported SNVs (V1-V3) upstream of *PRDM13*<sup>15</sup>. In addition to the previously  
135 reported V2 family 13<sup>15</sup>, two more NCMD families were found to harbour the variant V2  
136 (family 11 and the previously described MCDR1-linked family 12<sup>7</sup>).

137

138 ***Array-based comparative genomic hybridization (aCGH) uncovers duplications at the***  
139 ***MCDR3 locus in three NCMD families***

140 To investigate the MCDR3 locus for the presence of structural variants (SVs), an aCGH  
141 experiment using 10,000 probes spanning the region at chr5:11882-10140073  
142 (GRCh37/hg19) was performed in three affected individuals from families 1-3 which did  
143 not show linkage at the 6q16 locus (Supplementary Figs. S2-S4). All three families were  
144 found to harbour heterozygous duplications of approximately 45kb, downstream of *IRX1*  
145 and upstream of *ADAMTS16* (Fig. 2a). The duplications were found to be located in the  
146 minimal overlapping regions chr5:4391880-4434888 (GRCh37/hg19) in family 1 and  
147 chr5:4397221-4440150 (GRCh37/hg19) in families 2 and 3. These SVs were not seen in  
148 16 control individuals included in the same aCGH experiment, nor were they present in  
149 WGS data from 650 individuals with inherited retinal disease<sup>19</sup> or in publicly available  
150 population data (CNV browser)<sup>20</sup>.

151

152 ***WGS identifies four more NCMD families with duplications at the MCDR3 locus***

153 Thirteen affected individuals from families 1-7 underwent whole genome sequencing



154 (WGS). Graphical visualisation of individual paired-end reads using Integrative  
155 Genomics Viewer (IGV)<sup>21,22</sup> confirmed the presence of heterozygous tandem  
156 duplications in families 1-3 (Fig. 2b). Precise breakpoint coordinates were identified from  
157 coverage changes, split reads and chimeric reads. Family 1 had a 45158 bp duplicated  
158 region (GRCh37/hg19 chr5:4391377-4436535) and families 2 and 3 shared an identical  
159 43515 bp tandem duplication (GRCh37/hg19 chr5:4396927-4440442), overlapping the  
160 first identified SV by 85% of the sequence (GRCh37/hg19 chr5:4396925-4436534).  
161 Subsequently, members from families 4-7 were also found to carry the same 43 kb  
162 duplication.  
163 PCR primers were designed to amplify the novel sequence across the breakpoint between  
164 duplicated copies (Table 2, Fig. 3) and used to confirm the predicted breakpoints and  
165 assess segregation of the two variants in all available affected and unaffected members of  
166 families 1 and 2 (Fig. 3, Table 1 and Supplementary Fig. S1). PCR was then used to  
167 genotype the available affected individuals from families 3-7 and confirmed the presence  
168 of a band in all affected individuals tested (Table 1 and Supplementary Fig. S1).

169

170 ***Genotyping reveals three additional previously unmapped NCMD families with***  
171 ***duplications at the MCDR3 locus***

172 The remaining 8 unmapped families were tested with the established PCR assay for both  
173 duplications, and 3 of them (families 8-10) were also found to carry the 43 kb duplication  
174 (Table 1 and Supplementary Fig. S1). Thus, a total of 9 not knowingly related families  
175 were shown to harbour the same 43 kb tandem duplication at the MCDR3 locus. Five

176 affected members available from the remaining 5 families did not carry either of the two  
177 novel duplications.

178

179 ***Haplotype sharing analysis suggests presence of ancestral haplotypes at the MCDR1***  
180 ***and MCDR3 loci***

181 We hypothesized that finding the same 6q16 SNV and 5p15 duplication with identical  
182 breakpoint in 3 and 9 families respectively, could be due to two different shared ancestral  
183 haplotypes suggestive of a common founder, in keeping with previous reports on other  
184 6q16 NCMD families<sup>5,12,13,15</sup>. Therefore, haplotype sharing analysis was performed using  
185 available Illumina SNP array data from 14 affected individuals in 3 families carrying the  
186 6q16 V2 variant (families 11-13) and 14 affected individuals in 6 families carrying the  
187 5p15 43 kb duplication (families 2-7). Using a cut-off of 2.0 cM and 2.5 cM respectively,  
188 the results confirmed that all the genotyped 6q16 individuals collectively shared a RCHH  
189 of approximately 2.5 Mb from GRCh37/hg19 coordinate chr6:98962591 (rs150396) to  
190 chr6:101468591 (rs1321204) at the MCDR1 locus, and all the genotyped 5p15  
191 individuals collectively shared a RCHH of approximately 0.9 Mb from GRCh37/hg19  
192 coordinate chr5:4327455 (rs155354) to chr5:5210050 (rs1560063) at the MCDR3 locus  
193 (Supplementary Tabs. S1-S2 and Supplementary Figs. S9-S10).

194

195 **Discussion**

196

197 We report two distinct heterozygous tandem duplications at the MCDR3 locus in 30  
198 affected individuals from 10 NCMD families. The two novel SVs overlap the previously  
199 described duplication found in a single NCMD family of Danish origin<sup>15</sup> and further  
200 refine the 5p15 NCMD locus to a shared region of 39 kb in a gene desert downstream of  
201 *IRX1* and upstream of *ADAMTS16* (800 kb and 693.9 kb from the respective transcription  
202 start sites, Fig. 4).

203 We postulated that the 39 kb shared region could harbour *cis*-acting elements that  
204 contribute to the fine tuning of gene expression during macular development, affecting  
205 target gene expression spatially, temporally and/or quantitatively. Publicly available  
206 platforms were queried for informative data on gene expression and chromatin  
207 accessibility in relevant tissue types. A dataset screening for gene expression in fetal  
208 retina confirmed high expression of *IRX1* at 19-20 weeks of gestation in the macula, and  
209 medium expression levels in other regions (Supplementary Fig. S11). In contrast,  
210 *ADAMTS16* had medium expression levels throughout the retina<sup>23,24</sup>. Although no role in  
211 retinal pathophysiology has been described for *ADAMTS16*, the gene has high sequence  
212 similarity to *ADAMTS18* which has been previously associated with retinal disease<sup>32</sup>.  
213 Overall, the data suggest that the pattern and/or refined spatial dosage and timing of  
214 expression of the transcription factor *IRX1* may be important in macular development. A  
215 second dataset provided information on open chromatin conformation using DNase-  
216 accessible sequencing in fetal retina tissues at 5 stages from gestation day 72 to 125 (~10  
217 to 18 weeks)<sup>25</sup>. Different sites were identified to be open/active within the 39 kb shared

218 region at four out of five time points (~10-15 weeks of gestation) available during retinal  
219 development (Table 3). Interestingly, one of the sites was active during three  
220 developmental stages and the remaining four sites were functionally active as two  
221 overlapping pairs. At the last time point (day 125, ~18 weeks), all sites were  
222 inactive/closed. In the context of human macular development, the sites are active during  
223 the period where photoreceptors are proliferating and differentiating<sup>26</sup>; by week 14 of  
224 gestation, cells of the central retina exit mitosis<sup>26</sup>, corresponding to the period where  
225 DHSs are turning off.

226 As mentioned, the MCDR1 locus on chromosome 6q16 is associated with variants sited  
227 within a DHS, which suggests that aspects of macular development may be highly gene  
228 dosage sensitive. Exploring the function and precise target of such regulatory domains in  
229 both loci will be essential for understanding the disease mechanism of NCMD and  
230 investigating its potential role in the context of normal macular development. The graded  
231 expression of *IRX1* and known involvement in retinal development<sup>27,28</sup>, but not  
232 *ADAMTS16* in the macular region, suggests that *IRX1* is the probable target of the  
233 putative retinal regulatory element which, when duplicated, may cause misregulation of  
234 *IRX1*.

235 Eye development, like other organogenesis processes, requires the precise spatio-  
236 temporal and quantitative expression of genes, orchestrated by a complex network of  
237 regulatory mechanisms influencing critical transcription factors and other developmental  
238 genes. The lack of readily accessible animal or *in vitro* models has hindered detailed  
239 understanding of macular development, as this structure only evolved in higher primates  
240 among mammals. Recently, disrupted developmental expression of the transcription

241 factor and histone methyltransferase *PRDM13*<sup>29,30</sup> was suggested as a disease mechanism  
242 for NCMD at the 6q16 locus, based on the identification of non-coding SNVs and  
243 duplication events residing in an overlapping region upstream of *PRDM13* in many  
244 MCDR1 families. Differential regulation of *PRDM13* in eyecups derived from wild-type  
245 iPSCs<sup>15,16</sup> was suggested. However, no causal relationship between the non-coding  
246 variants and *PRDM13* expression has been identified.

247 Despite variable presentation in affected individuals, the NCMD phenotypic spectrum is  
248 indistinguishable in patients assigned to either of the two linked loci, MCDR1 and  
249 MCDR3. Whether a biological and functional connection between *PRDM13* at the  
250 MCDR1 locus and the most likely candidate gene *IRX1* at the MCDR3 locus exists  
251 warrants further investigation. iPSC technology and CRISPR manipulation in eye cups  
252 from normal and affected individuals may help elucidate the molecular mechanism<sup>33,34</sup>  
253 and the potential molecular links between the two genes. Importantly, the involvement of  
254 ancestral variation at both the 6q16 and 5p15 loci (Supplementary Figs. S9-S10) in such a  
255 highly penetrant dominant disease is intriguing, with the implication that there may exist  
256 a significant number of unrecognized related NCMD families. Full clinical examination  
257 reveals a high degree of penetrance, but visually unaffected individuals in whole families  
258 may fail to be ascertained.

259 Finally, the two novel duplications identified in this study significantly further the  
260 understanding of the molecular genetics of NCMD at the MCDR3 locus and provide  
261 additional effective tools for the molecular diagnosis of NCMD families.

262

## 263 **Materials and Methods**

264

### 265 *Families*

266 All families were ascertained at Moorfields Eye Hospital, London, United Kingdom,  
267 expect for family 1<sup>14</sup> (Vision Centre, Children's Clinical University Hospital, Riga,  
268 Latvia) and family 13<sup>9</sup> (Centre Hospitalier Régional Universitaire de Lille, France).  
269 When possible, retinal imaging was undertaken using colour fundus photography, fundus  
270 autofluorescence and OCT imaging. Blood/saliva samples were collected for DNA  
271 extraction, genotyping and sequence analyses. The study protocol was approved by the  
272 local ethics committees (Central Medical Ethics Committee of Latvian Republic; NRES  
273 Committee London – Camden & Islington) and conformed to the tenets of the  
274 Declaration of Helsinki. Written informed consent was obtained from all participants, or  
275 their parents, before inclusion in the study.

276

### 277 *Genotyping*

278 Genomic DNA was extracted from whole blood/saliva and genotyped using the Illumina  
279 HumanOmniExpress-24 v1.0 beadchip (Illumina, Inc., San Diego, CA, USA). Genotypes  
280 were determined using the Genotyping Module in the Illumina GenomeStudio v2011.1  
281 software.

282

### 283 *Haplotype sharing analysis*

284 In order to search for chromosomal segments sharing the same haplotype across affected  
285 individuals (within the same family or across different families), the non-parametric HH  
286 method<sup>18</sup> was used for the analysis of those affected individuals that were genotyped with

287 the Illumina array. The HH is a type of haplotype described by the homozygous SNPs  
288 only (all heterozygous SNPs are removed) and, therefore, can be uniquely determined on  
289 each chromosome. Since affected family members who inherited the same mutation from  
290 a common ancestor share a chromosomal segment IBD around the disease gene, they  
291 should not have discordant homozygous calls in the IBD region and thus they should  
292 share the same HH. The HH approach predicts IBD regions through the identification of  
293 RCHHs defined as those regions with a shared HH among affected individuals and a  
294 genetic length longer than a certain cut-off value (recommended cut-off for Illumina  
295 HumanOmniExpress array is 2.5/3.0 cM for the analysis of one single family).

296

### 297 *aCGH*

298 aCGH was performed at Oxford Gene Technology (OGT) (Begbroke, United Kingdom)  
299 using a custom design consisting of 10,000 probes spanning the MCDR3 locus at  
300 GRCh37/hg19 chr5:11882-10140073 (approximately 1 probe every 1,000 bp), designed  
301 with Agilent e-Array software (Agilent Technologies Inc., Santa Clara, CA, USA), in  
302 three individuals from families 1-3 (Supplementary Fig. S1). Sixteen other individuals  
303 affected by non-ocular phenotypes were also included in the experiment and used as  
304 controls in the analysis. Scanned images of the arrays were processed with OGT  
305 CytoSure™ Interpret Software v4.4 using the Accelerate Workflow for calling CNVs.  
306 Duplications or deletions were considered when the  $\log_2$  ratio of the Cy3/Cy5 intensities  
307 of a region encompassing at least four probes was  $> 0.3$  or  $< -0.6$ , respectively (software  
308 default settings).

309

### 310 ***WGS and bioinformatics analysis***

311 Whole-genome sequencing was performed using the Illumina HiSeq X10 platform  
312 (Illumina, Inc., San Diego, CA, USA), generating minimum coverage of 30X. Reads  
313 were aligned to the hg19 human reference sequence (build GRCh37) with novoalign  
314 (version 3.02.08). The aligned reads were sorted by base pair position and duplicates  
315 were marked using novosort. Discordant reads were marked with samblaster (version  
316 0.1.20) and sent to a separate file for manual inspection of breakpoints using the IGV  
317 (version 2.3.61). SVs were manually investigated using the IGV by identifying peaks of  
318 discordant reads which were interpreted as breakpoints. The identified duplicated regions  
319 were also screened for the presence of common copy number variants using data from the  
320 CNV browser<sup>20</sup> ([https://personal.broadinstitute.org/handsake/mcnv\\_data/](https://personal.broadinstitute.org/handsake/mcnv_data/)) and WGS data  
321 from 650 individuals with inherited retinal disease<sup>19</sup>.

322

### 323 ***Sanger sequencing validation of duplication events***

324 Segregation analysis of the duplication events identified by WGS was performed using  
325 primers (Table 2) designed to span the end of first copy and start of second copy. A  
326 graphical representation is shown in Fig. 3. After sequence confirmation with Sanger  
327 sequencing, PCR was used to genotype selected individuals from all identified families.

328

### 329 ***In silico analysis of duplicated sequences and expression of flanking genes***

330 The Encyclopedia of DNA Elements (ENCODE)<sup>25</sup> was interrogated for fetal retina  
331 datasets of interest. Bed files from DNA-seq datasets (ENCFF249FGP, ENCFF937NUZ,  
332 ENCFF401BCF, ENCFF591NRB, ENCFF265ZNN, Stamatoyannopoulos' laboratory)



333 were downloaded and investigated at the shared duplicated region with R Studio. A  
334 second microarray expression dataset on human fetal retina (19-20 gestation week) was  
335 queried for the genes of interest<sup>24</sup> using the platform GENEVESTIGATOR<sup>23</sup>.

## 336 References

- 337 1. Provis, J. M., Dubis, A. M., Maddess, T. & Carroll, J. Progress in Retinal and Eye  
338 Research Adaptation of the central retina for high acuity vision: Cones, the  
339 fovea and the avascular zone. *Prog. Retin. Eye Res.* **35**, 63–81 (2013).
- 340 2. Yang, Z. *et al.* Clinical characterization and genetic mapping of North Carolina  
341 macular dystrophy. *Vision Research* **48**, 470–477 (2008).
- 342 3. Rosenberg, T. *et al.* Clinical and genetic characterization of a Danish family with  
343 North Carolina macular dystrophy. *Mol. Vis.* **16**, 2659–2668 (2010).
- 344 4. Small, K. W. *et al.* North Carolina macular dystrophy is assigned to chromosome  
345 6. *Genomics* **13**, 681–685 (1992).
- 346 5. Pauleikhoff, D. *et al.* Clinical and genetic evidence for autosomal dominant North  
347 Carolina macular dystrophy in a German family. *American Journal of*  
348 *Ophthalmology* **124**, 412–415 (1997).
- 349 6. Rabb, M. F., Mullen, L., Yelchits, S., Udar, N. & Small, K. W. A North Carolina  
350 macular dystrophy phenotype in a Belizean family maps to the MCDR1 locus. *Am.*  
351 *J. Ophthalmol.* **125**, 502–8 (1998).
- 352 7. Reichel, M. B. *et al.* Phenotype of a British North Carolina macular dystrophy  
353 family linked to chromosome 6q. *Br. J. Ophthalmol.* **82**, 1162–1168 (1998).
- 354 8. Rohrschneider, K., Blankenagel, A., Kruse, F. E., Fendrich, T. & Völcker, H. E.  
355 Macular function testing in a German pedigree with North Carolina macular  
356 dystrophy. *Retina* **18**, 453–9 (1998).
- 357 9. Small, K. W., Puech, B., Mullen, L. & Yelchits, S. North Carolina macular  
358 dystrophy phenotype in France maps to the MCDR1 locus. *Mol. Vis.* **3**, 1 (1997).
- 359 10. Small, K., Garcia, C., Gallardo, G., Udar, N. & Yelchits, S. North Carolina  
360 macular dystrophy (MCDR1) in Texas. *Retina* **18**, 448–452 (1998).
- 361 11. Michaelides, M. *et al.* An early-onset autosomal dominant macular dystrophy  
362 (MCDR3) resembling North Carolina macular dystrophy maps to chromosome 5.  
363 *Investig. Ophthalmol. Vis. Sci.* **44**, 2178–2183 (2003).
- 364 12. Sauer, C. G. *et al.* An ancestral core haplotype defines the critical region  
365 harbouring the North Carolina macular dystrophy gene (MCDR1). *J. Med. Genet.*  
366 **34**, 961–966 (1997).
- 367 13. Small, K. W. North Carolina macular dystrophy: clinical features, genealogy, and  
368 genetic linkage analysis. *Trans. Am. Ophthalmol. Soc.* **96**, 925–961 (1998).
- 369 14. Audere, M. *et al.* Genetic linkage studies of a North Carolina macular dystrophy  
370 family. *Medicina (Kaunas)*. **52**, 180–186 (2016).
- 371 15. Small, K. W. *et al.* North Carolina Macular Dystrophy Is Caused by Dysregulation  
372 of the Retinal Transcription Factor PRDM13. *Ophthalmology* **123**, 9–18 (2016).
- 373 16. Bowne, S. J. *et al.* North Carolina macular dystrophy (MCDR1) caused by a novel  
374 tandem duplication of the PRDM13 gene. *Mol. Vis.* **22**, 1239–1247 (2016).
- 375 17. MacDonald, J. R., Ziman, R., Yuen, R. K. C., Feuk, L. & Scherer, S. W. The  
376 Database of Genomic Variants: A curated collection of structural variation in the  
377 human genome. *Nucleic Acids Res.* **42**, (2014).
- 378 18. Miyazawa, H. *et al.* Homozygosity haplotype allows a genomewide search for the  
379 autosomal segments shared among patients. *Am. J. Hum. Genet.* **80**, 1090–102  
380 (2007).

- 381 19. Carss, K. J. *et al.* Comprehensive Rare Variant Analysis via Whole-Genome  
382 Sequencing to Determine the Molecular Pathology of Inherited Retinal Disease.  
383 *Am. J. Hum. Genet.* **100**, 75–90 (2017).
- 384 20. Handsaker, R. E. *et al.* Large multiallelic copy number variations in humans. *Nat.*  
385 *Genet.* **47**, 1–10 (2015).
- 386 21. Robinson, J. T. *et al.* Integrative genomics viewer. *Nat. Biotechnol.* **29**, 24–26  
387 (2011).
- 388 22. Thorvaldsdóttir, H., Robinson, J. T. & Mesirov, J. P. Integrative Genomics Viewer  
389 (IGV): High-performance genomics data visualization and exploration. *Brief.*  
390 *Bioinform.* **14**, 178–192 (2013).
- 391 23. Hruz, T. *et al.* Genevestigator V3: A Reference Expression Database for the Meta-  
392 Analysis of Transcriptomes. *Adv. Bioinformatics* **2008**, 1–5 (2008).
- 393 24. Kozulin, P. & Provis, J. M. Differential gene expression in the developing human  
394 macula: Microarray analysis using rare tissue samples. *J. Ocul. Biol. Dis. Infor.* **2**,  
395 176–189 (2009).
- 396 25. Dunham, I. *et al.* An integrated encyclopedia of DNA elements in the human  
397 genome. *Nature* **489**, 57–74 (2012).
- 398 26. Provis, J. M., van Driel, D., Billson, F. A. & Russell, P. Development of the  
399 human retina: patterns of cell distribution and redistribution in the ganglion cell  
400 layer. *J. Comp. Neurol.* **233**, 429–51 (1985).
- 401 27. Choy, S. W. *et al.* A cascade of *irx1a* and *irx2a* controls *shh* expression during  
402 retinogenesis. *Dev. Dyn.* **239**, 3204–3214 (2010).
- 403 28. Cheng, C. W., Yan, C. H. M., Hui, C. chung, Strähle, U. & Cheng, S. H. The  
404 homeobox gene *irx1a* is required for the propagation of the neurogenic waves in  
405 the zebrafish retina. *Mech. Dev.* **123**, 252–263 (2006).
- 406 29. Watanabe, S. *et al.* Prdm13 regulates subtype specification of retinal amacrine  
407 interneurons and modulates visual sensitivity. *J. Neurosci.* **35**, 8004–20 (2015).
- 408 30. Hanotel, J. *et al.* The Prdm13 histone methyltransferase encoding gene is a Ptf1a-  
409 Rbpj downstream target that suppresses glutamatergic and promotes GABAergic  
410 neuronal fate in the dorsal neural tube. *Dev. Biol.* **386**, 340–357 (2014).
- 411 31. Cavodeassi, F., Modolell, J. & Gómez-Skarmeta, J. L. The Iroquois family of  
412 genes: from body building to neural patterning. *Development* **128**, 2847–2855  
413 (2001).
- 414 32. Chandra, A. *et al.* Expansion of ocular phenotypic features associated with  
415 mutations in ADAMTS18. *JAMA Ophthalmol.* **132**, 996–1001 (2014).
- 416 33. Zhong, X. *et al.* Generation of three-dimensional retinal tissue with functional  
417 photoreceptors from human iPSCs. *Nat. Commun.* **5**, 4047 (2014).
- 418 34. Schwarz, N. *et al.* Translational read-through of the RP2 Arg120stop mutation in  
419 patient iPSC-derived retinal pigment epithelium cells. *Hum. Mol. Genet.* **24**, 972–  
420 86 (2015).
- 421

422 **Figure legends**

423

424 **Figure 1 NCMD typical clinical presentation in two selected individuals from family**  
425 **3 (IV:5) and family 2 (IV:5).** Each panel shows fundus autofluorescence and optical  
426 coherence tomography (OCT) images. Individual IV:5 (a,b) from family 3 shows a mild  
427 form of disease with relatively symmetrical, bilateral hyperfluorescent drusen-like  
428 deposits concentrated within the macular region and an otherwise normal OCT.  
429 Individual IV:3 (c,d) from family 2 presents with a well demarcated, relatively  
430 symmetrical and bilateral area of macular chorioretinal atrophy.

431

432 **Figure 2 NCMD is caused by intergenic duplication events located between *IRX1***  
433 **and *ADAMTS16*.** (a) aCGH experiment (10,000 probes spanning the MCDR3 locus at  
434 GRCh37/hg19 chr5:11882-10140073, panel I) performed in three affected individuals  
435 from families 1-3 that were found to harbour heterozygous duplications of approximately  
436 43 kb (panel II) located in a gene desert downstream of *IRX1* and upstream of  
437 *ADAMTS16* (panel III), also confirmed by WGS (b) by changes in coverage from  
438 concordant and discordant reads (panel I and II, respectively) and identification of  
439 chimeric reads, pair-reads with opposing orientation (displayed in green, panel III).  
440 Panels are presented with a split view option within IGV. The duplications are located in  
441 the overlapping regions GRCh37/hg19 chr5:4391880-4434888 (family 1) and  
442 GRCh37/hg19 chr5:4397221-4440150 (families 2 and 3).

443

444 **Figure 3 PCR and Sanger sequencing validation of duplication breakpoints and**  
445 **segregation in family 1 (a) and family 2 (b).** All available individuals (Supplementary  
446 Fig. S1) were tested with primers designed across the predicted breakpoints to generate a  
447 unique junction fragment sequence. The exact breakpoint is marked with a red bar; PCR  
448 primers are represented with blue arrows. L = ladder; W = water; “-“ = genomic DNA  
449 pooled from control individuals.

450

451 **Figure 4 Schematic representation of the MCDR3 locus which is refined to a 39 kb**  
452 **shared genomic region (GRCh37/hg19 chr5:4396925-4436534).** The shared sequence  
453 between a previously reported duplication and the two novel SVs identified in this study  
454 is located in a large gene desert, downstream of *IRX1* and upstream of *ADAMTS16*, 800  
455 kb and 693.9 kb from their respective transcription start sites. Publicly available NGS  
456 datasets were queried for informative data on chromatin accessibility and 3 sites were  
457 found active from human gestation day 72 to 105 in fetal retina, suggestive of functional  
458 acting elements within this site.

459

#### 460 **Acknowledgements**

461 The authors would like to acknowledge the ENCODE Consortium and  
462 Stamatoyannopoulos' laboratory for generating the DNA-seq datasets queried in this  
463 study, the NIHR BioResource - Rare Disease Consortium (Dr. Keren J Carss and Prof. F  
464 Lucy Raymond) for access to CNV data from WGS data, Dr. Gabriela E Jones  
465 (University Hospitals of Leicester NHS Trust, Leicester, UK) for help with patient  
466 recruitment, Dr. V. Plagnol (UCL Genetics Institute, London, UK) for access to control

467 aCGH data, and UCL Computer Science Cluster and Technical Support (London, UK).  
468 This work was supported by grants from the NIHR Biomedical Research Centre at  
469 Moorfields Eye Hospital National Health Service Foundation Trust and UCL Institute of  
470 Ophthalmology (London, UK), the Research to Prevent Blindness (USA), the British Eye  
471 Research Foundation (UK), Fight for Sight (UK), the Macular Society (UK), Moorfields  
472 Eye Hospital Special Trustees (UK), Moorfields Eye Charity (UK), the Foundation  
473 Fighting Blindness (USA) and Retinitis Pigmentosa Fighting Blindness (UK). RSS is  
474 funded through a Fight for Sight PhD studentship granted to ARW and VvH. The views  
475 expressed in this publication are those of the authors and not necessarily those of the  
476 funding bodies.

477

#### 478 **Author Contributions Statement**

479 Study conception and design: ATM, ARW, VvH, VC, RSS, GA.

480 Patient recruitment and phenotyping: ATM, ARW, AK, MM, BP, BL, SV.

481 Acquisition of data: VC, RSS, GA, II, MA, KR.

482 Analysis and/or interpretation of data: VC, RSS, NP, GA.

483 Drafting of manuscript: VC, RSS.

484 Critical revision for important intellectual content: ATM, ARW, VvH, GA.

485 All authors have read and accepted the final version of the manuscript.

486

#### 487 **Additional Information**

##### 488 **Competing financial interests**

489 The authors declare no competing financial interests.

## Tables

**Table 1** Summary of families with two newly reported tandem duplications at the MCDR3 locus and previously identified V2 variant at the MCDR1 locus.

Family number	Family ID	Origin	Phenotype	Experimental procedure	Causative allele change	Nucleotide change	Number of affected family members analysed	Number of unaffected family members analysed	Total number of family members analysed
1	GC19806 <sup>14</sup>	Latvian	NCMD	SNP, aCGH, WGS, PCR/Sanger	chr5:4391377-4436535	45158 bp duplication	5	1	
2	GC15626 <sup>11</sup>	British	NCMD	SNP, aCGH, WGS, PCR/Sanger	chr5:4396927-4440442	43515 bp duplication	9	8	
3	GC15119	British	NCMD	SNP, aCGH, WGS, PCR/Sanger	chr5:4396927-4440442	43515 bp duplication	4	0	
4	GC13840	British	NCMD	SNP, WGS, PCR/Sanger	chr5:4396927-4440442	43515 bp duplication	3	0	
5	GC19075	British	NCMD	SNP, WGS, PCR/Sanger	chr5:4396927-4440442	43515 bp duplication	3	0	
6	GC15475	British	NCMD	SNP, WGS, PCR/Sanger	chr5:4396927-4440442	43515 bp duplication	1	0	
7	GC11709	British	NCMD	SNP, WGS, PCR/Sanger	chr5:4396927-4440442	43515 bp duplication	1	0	
8	GC16913	British	NCMD	PCR/Sanger	chr5:4396927-4440442	43515 bp duplication	1	0	
9	GC4092	British	NCMD	PCR/Sanger	chr5:4396927-4440442	43515 bp duplication	1	0	
10	GC23501	British	NCMD	PCR/Sanger	chr5:4396927-4440442	43515 bp duplication	2	1	
11	GC15416	British	NCMD	SNP, PCR/Sanger	chr6:100040987	G>C (V2)	2	0	
12	GC3722 <sup>7</sup>	British	NCMD	SNP, PCR/Sanger	chr6:100040987	G>C (V2)	12	8	
13	GC17225 <sup>9,15</sup>	French	NCMD	SNP, PCR/Sanger	chr6:100040987	G>C (V2)	12	15	
						<b>Total</b>	<b>56</b>	<b>33</b>	

Genomic coordinates refer to GRCh37/hg19 assembly. SNP, aCGH, WGS, PCR/Sanger indicate Illumina SNP array, array-based comparative genomic hybridization, whole-genome sequencing and Sanger Sequencing, respectively. Five affected members from five additional NCMD families were also tested for the presence of previously reported SNVs V1-V3<sup>15</sup> and the two tandem duplications found in this study, but none of these affected individuals was found to carry any of the variants.

**Table 2** Primer sequences used for the segregation analysis of the two novel MCDR3 duplications identified in the study.

<b>Duplication size</b>	<b>Primer sequence</b>		<b>Tm (°C)</b>	<b>Length (bp)</b>
43 kb	F	5' - TTGTGGACTGAGCAAGCAAG - 3'	63	532
	R	5' - GGAGCAGAAGTTAAATGTGGAGA - 3'		
45 kb	F	5' - TTTGCTTGATCAATTCTGCTG - 3'	63	500
	R	5' - TTCTCAGTTGGAAGAGCACAAA - 3'		

Tm=Temperature of melting.

**Table 3** DHSs active during fetal retina development at the 39 kb shared duplicated region (GRCh37/hg19 chr5:4396925-4436534).

<b>Chromosome</b>	<b>Start position</b>	<b>End position</b>	<b>Gestation day (fetal retina)</b>
5	4418340	4418490	74
5	4420820	4420970	74, 89, 103
5	4418320	4418470	85
5	4420860	4421010	85
5	4409260	4409410	103

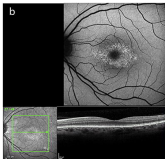
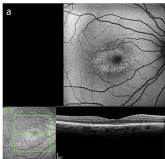
Gestation day 125 shows no active site at the 39 kb shared region. The fetal retina datasets were available from ENCODE<sup>25</sup>, produced by the Stamatoyannopoulos' laboratory.



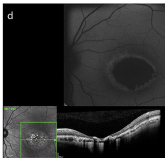
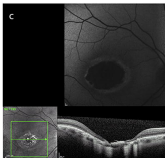
Right eye (OD)

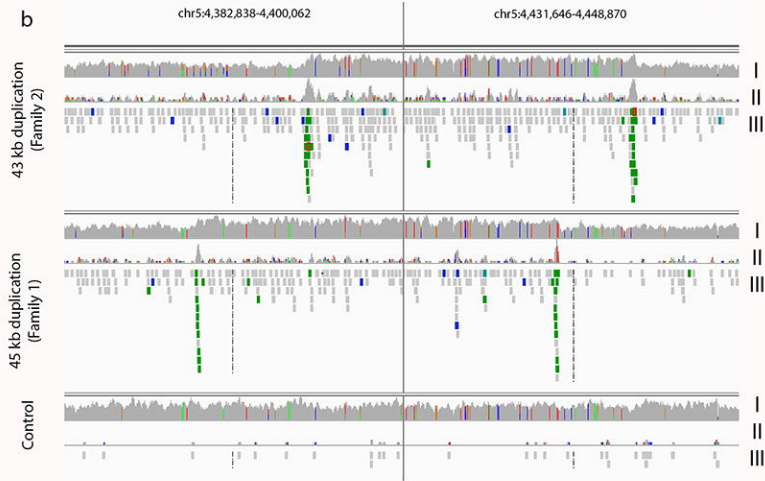
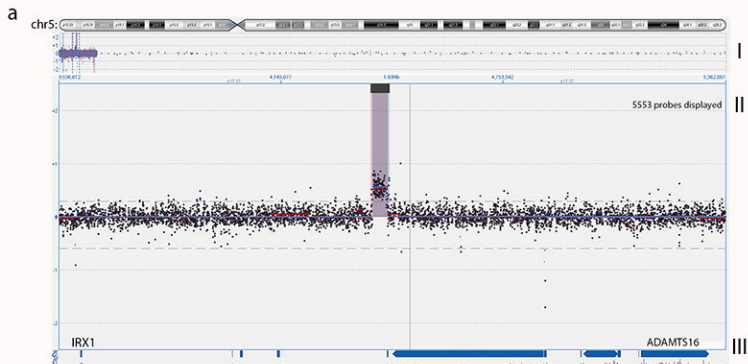
Left eye (OS)

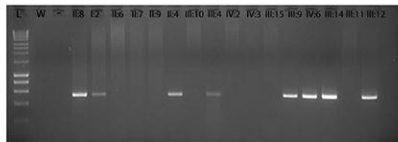
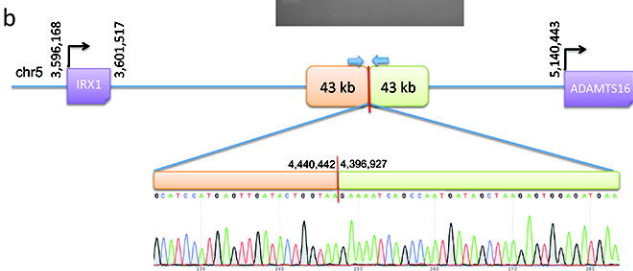
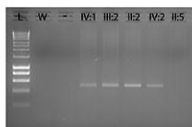
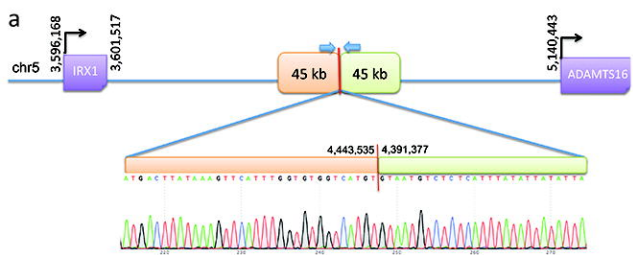
Family 3: IV:3



Family 2: IV:5







Coding gene

lncRNA  
RP11-445O3

Predicted enhancers

Predicted insulators

Tandem duplication

★ DHS active in fetal retina

